Supporting Information for:

Avoidance of Density Anomalies as a Structural Principle for Semicrystalline Polymers: The Importance of Chain Ends and Chain Tilt

Keith J. Fritzsching[1], Kanmi Mao[2], Klaus Schmidt-Rohr[1]*

[1]: Department of Chemistry, Brandeis University, Waltham, 415 South St, MA 02453, USA

[2]: ExxonMobil Research and Engineering, 1545 Route 22 East, Annandale, NJ 08801, USA

Submitted to *Macromolecules*

Table of Contents

Section	*Page*
Density profiles for self-avoiding tight folds	2
High–temperature SEC of HDPE40k	3
Quantitative solid-state NMR of HDPE40k	4
High-temperature SEC of HDPE7k	5
Quantitative solid-state NMR of HDPE7k	5
Quantitative solid-state NMR of Pwax3k	6
Graphical description of chain-fold algorithm	7
Direct-polarization spectra of HDPE7k with 2-s recycle delays	8
Scattering patterns of crystalline chains aligned with the machine direction	9
Straight-chain fold with excluded volume	10

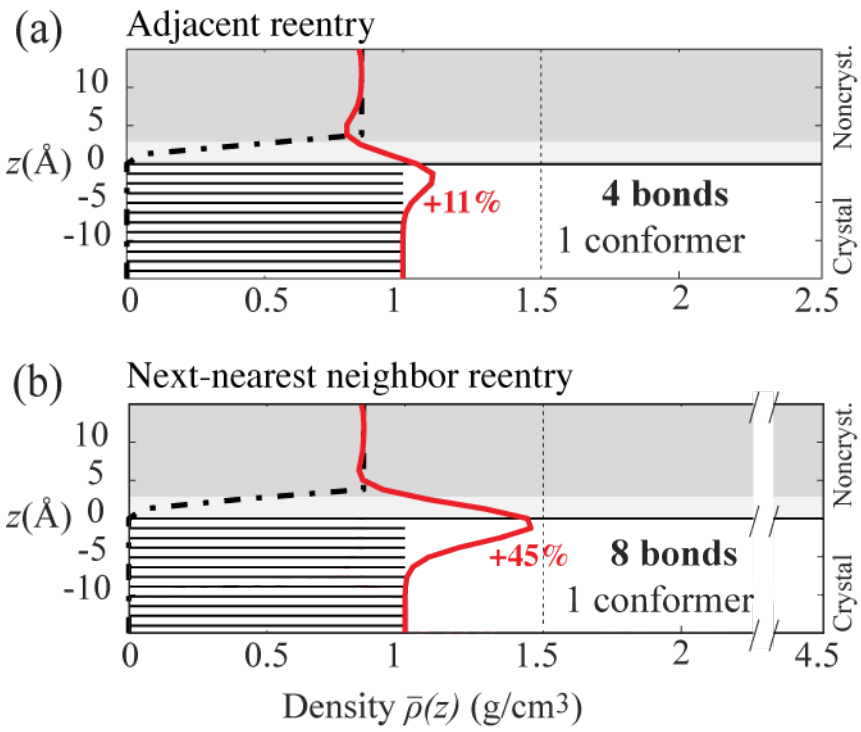

Figure S1. Density profiles of self-avoiding folds of minimal length on a diamond lattice for (a) adjacent reentry and (b) next-nearest neighbor reentry. These loops are unrealistically short[18] but have been included to show that excess density results even in these extreme cases. Profiles for more realistic loops are shown in Figure 2. Red line: Density profile after Gaussian sampling of 0.6 nm width (fwhm). See Figure S9 for consideration of the excluded volume.

High-temperature size exclusion chromatography. High-temperature size exclusion chromatography (or gel permeation chromatography) of the 5% ^{13}C-^{12}C HDPE sample was performed by Creative Proteomics (Shirley, NY). The HDPE was dissolved in 1,3,5-trichlorobenzene at 160 °C, at a concentration of 0.10 mg/mL with 0.0125% BHT. A 200 μL aliquot of this solution was injected into a 3 x pL Olexis column, eluted at a rate of 1.00 mL per minute and analyzed with a differential refractive index (RI) detector. The column was heated to 150 °C throughout the analysis. The molecular weight distribution was calculated based on commercial polystyrene standards. The data, reanalyzed with a carefully selected baseline, are shown in Fig. S2. The molecular weights obtained in our reanalysis were M_w = 300 ± 100 kg/mol and M_n = 50 ± 20 kg/mol, the latter consistent with ^{13}C NMR (40 ± 10 kg/mol).

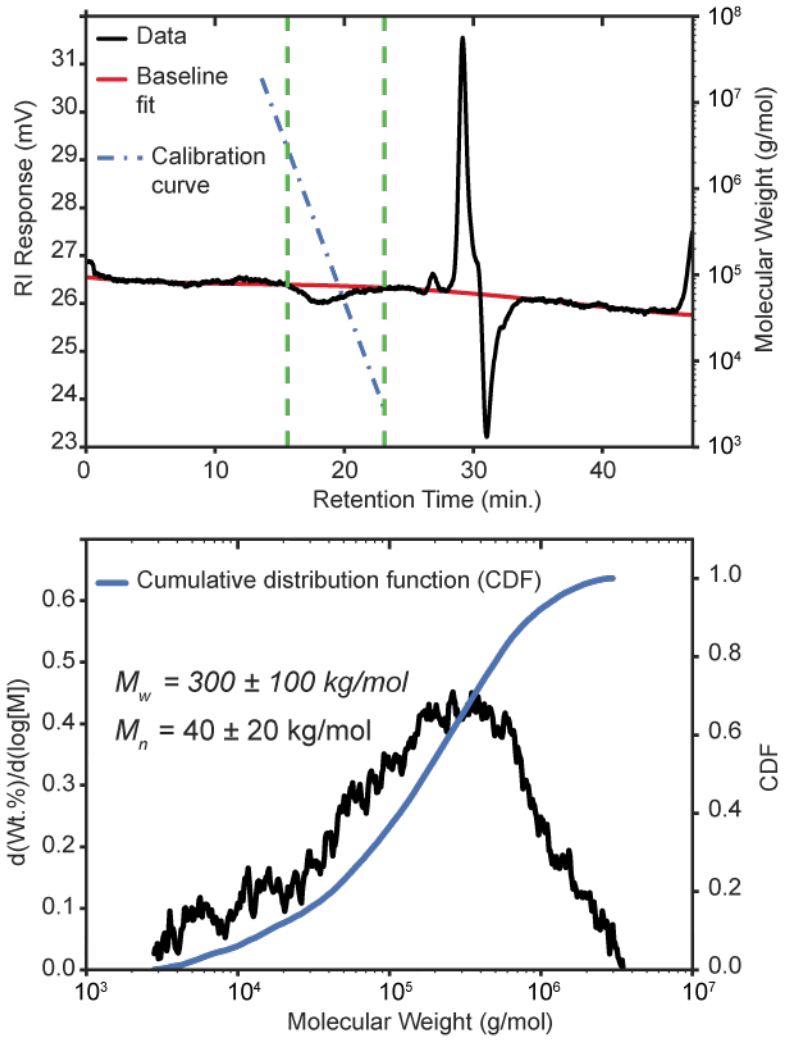

Figure S2. High-temperature size exclusion chromatography of the 5% ^{13}C-^{12}C HDPE (HDPE40k).

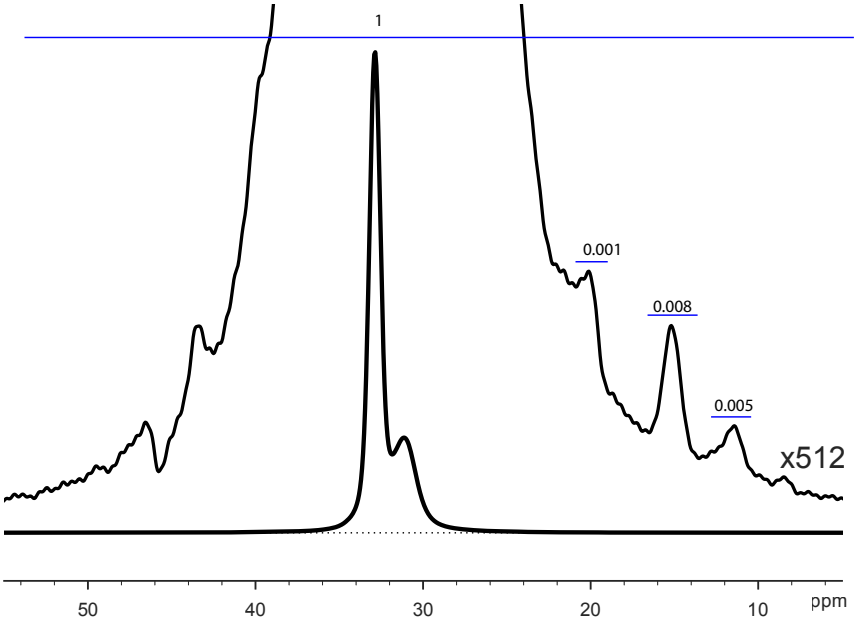

Figure S3. Quantitative solid-state ^{13}C NMR spectrum of HDPE40k, acquired using multiCP at 4.5 kHz MAS. Peak integrals (after baseline correction) are given above the methyl peaks; the total integral of the spectrum is 1.0.

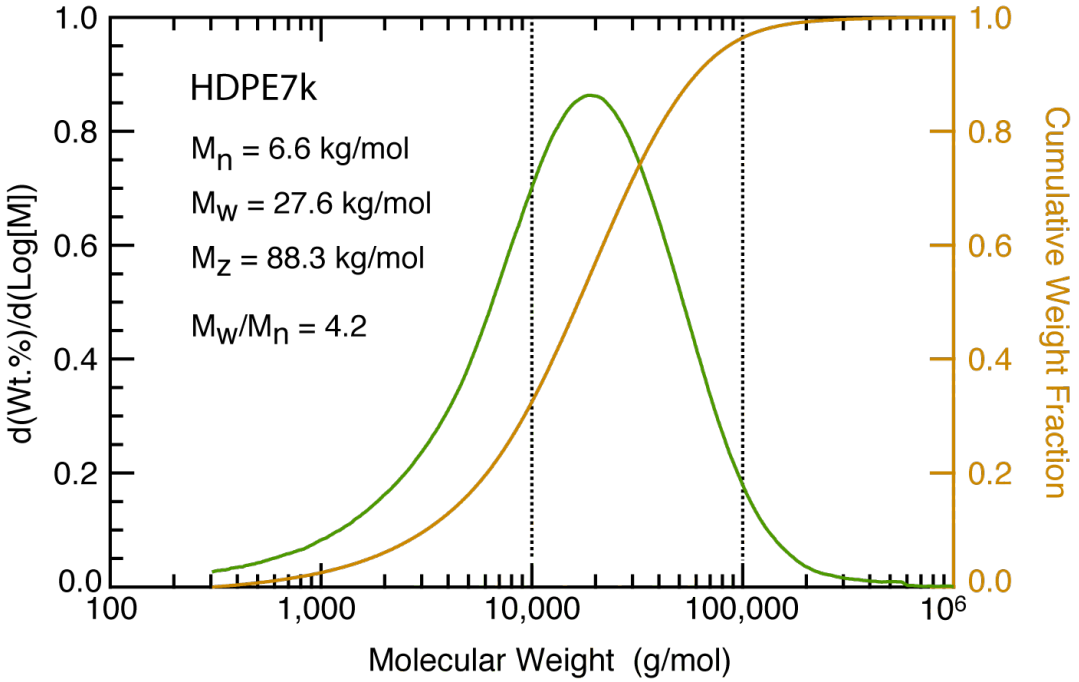

Figure S4. Molecular weight distribution from high-temperature size exclusion chromatography of HDPE7k, courtesy of ExxonMobil Research & Engineering.

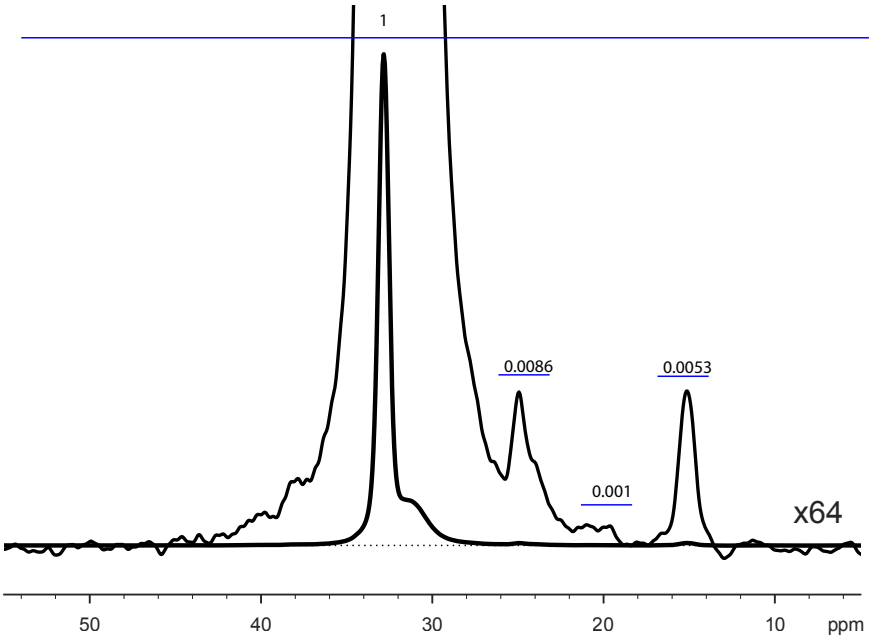

Figure S5. Quantitative solid-state ^{13}C NMR spectrum of HDPE7k, acquired using multiCP at 4.5 kHz MAS. Peak integrals are given above the methyl and (ω-1) CH_2 peaks; the total integral of the spectrum is 1.0.

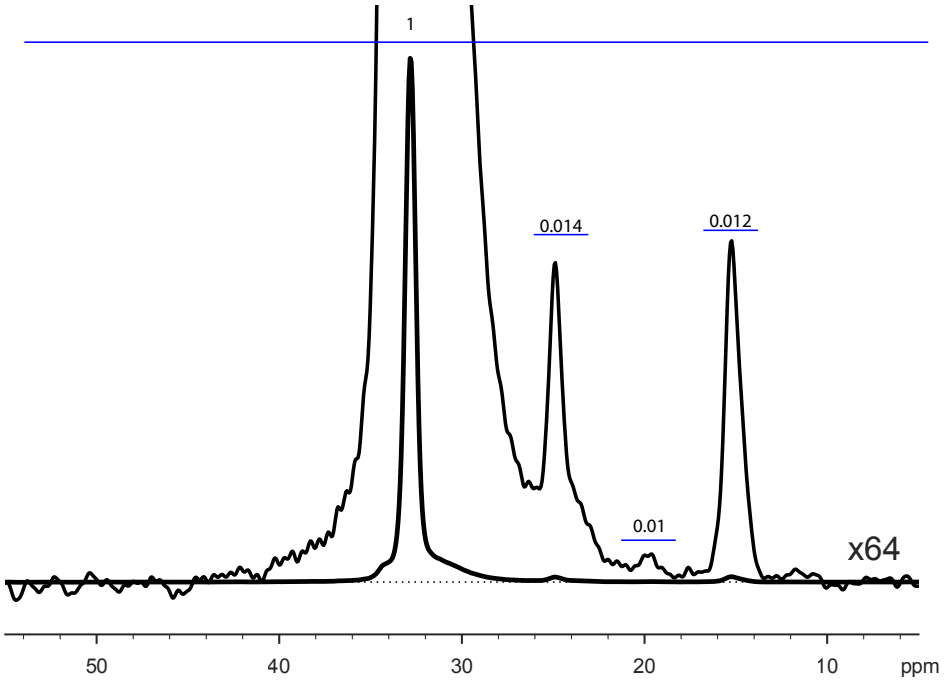

Figure S6. Quantitative solid-state ^{13}C NMR spectrum of Pwax3k, acquired using multiCP at 4.5 kHz MAS. Peak integrals are given above the methyl and (ω-1) CH_2 peaks; the total integral is 1.0.

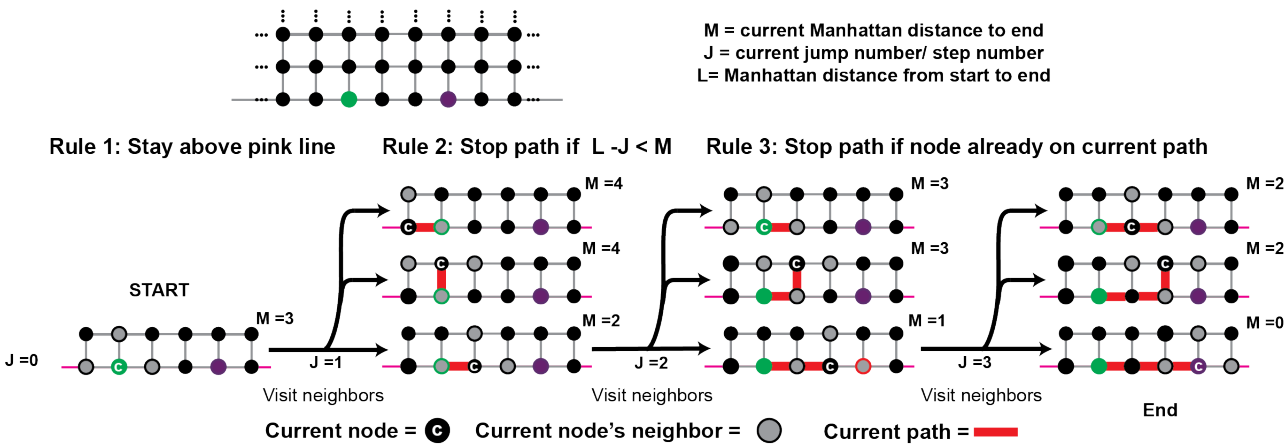

Figure S7. A graphical description of the modified breadth-first search algorithm used to identify all possible non-cyclic loops on a non-directional graph. The process is depicted on a square lattice for easier visualization.

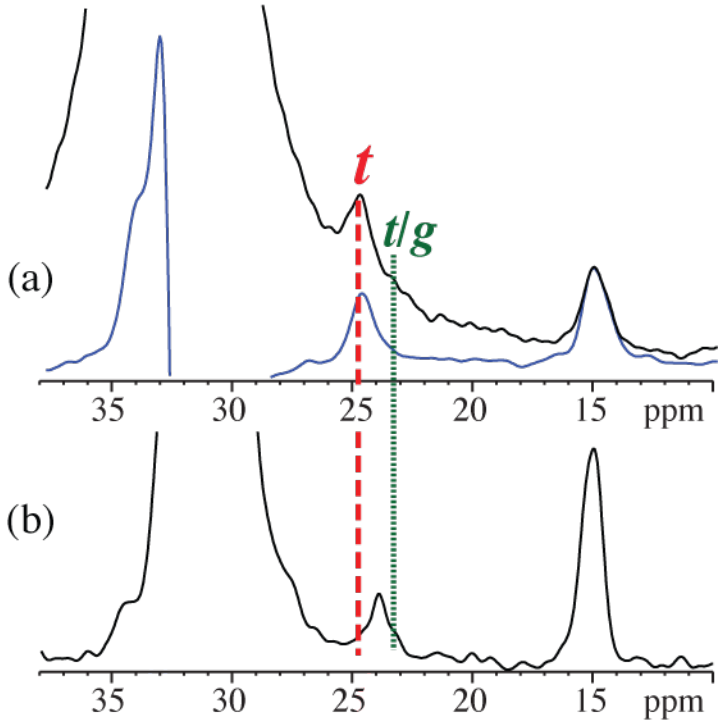

Figure S8. NMR evidence for chain ends in the crystallites of HDPE7k, from conformation-dependent ^{13}C chemical shifts of near-terminal (ω-1) CH_2 groups (M_n = 6.6 kg/mol, M_w = 28 kg/mol). (a) Comprehensive spectrum of the crystalline components after a 1-s T_{1C} filter. In the lower-trace spectrum (blue line), background from crystalline and amorphous backbone carbons has been suppressed by a chemical-shift filter and 1-s T_{1C} filter, respectively. (b) Spectrum of the most mobile segments, selected by direct polarization and dipolar dephasing; note that the CH_3 resonance contains strong contributions from crystalline chain ends, due to motional averaging of dipolar couplings by the CH_3 rotational jumps.

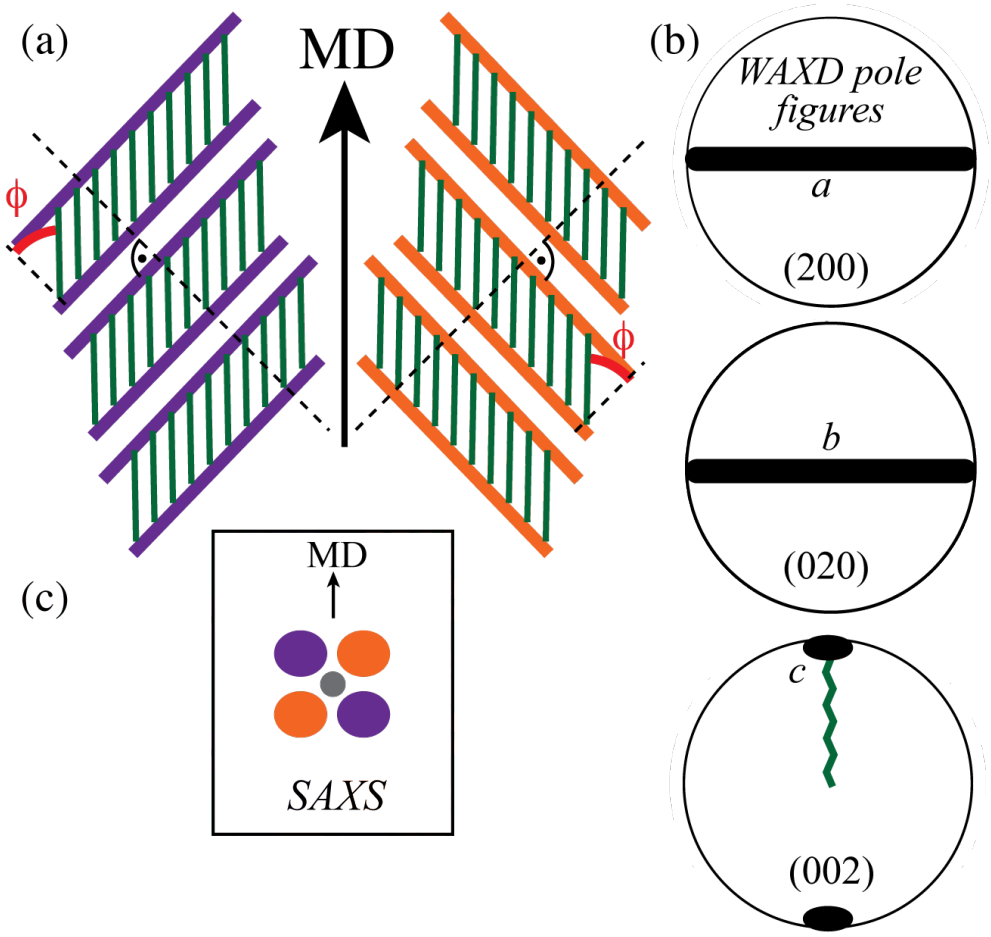

Figure S9. Characteristic scattering patterns of crystalline PE lamellae with crystalline chains macroscopically aligned along the machine direction and tilted relative to the lamellar normal by an angle ϕ. (a) Structural cartoon of the morphology. While (b) the resulting WAXD pole figures of the (200), (020), and (002) directions in PE are very simple, (c) SAXS shows a four-point pattern due to the tilted stacks of lamellae.

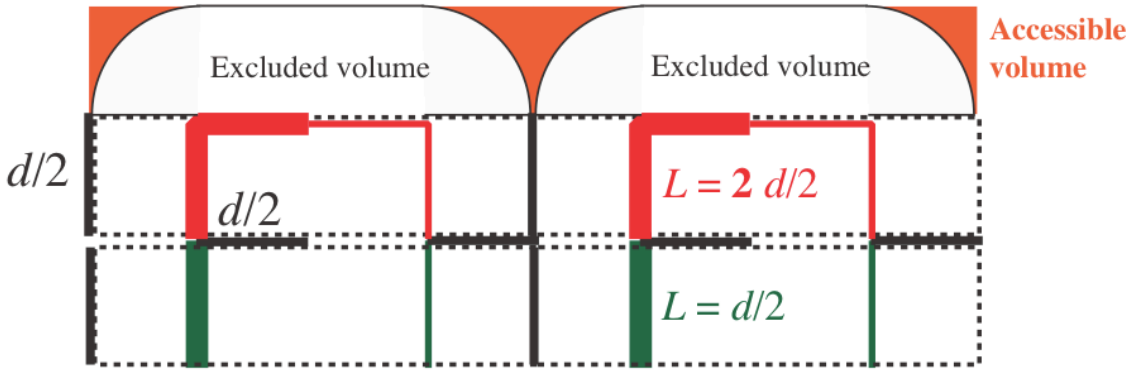

Figure S10. Straight-chain fold with excluded volume, which overall nearly cancels the density doubling in the fold, which nevertheless produces a persistent local density anomaly, see Figure 2(b). The net increase in density is due to the "accessible volume" (highlighted in orange) available to other chains. The lengths of loops and chain stems can be measured conveniently in Adobe Illustrator (Window, Document Info, Object; Paths: shows length in points).